Global simulations of protoplanetary discs
with Ohmic resistivity and ambipolar diffusion

Oliver Gressel *
Niels Bohr International Academy (NBIA), Copenhagen

Richard P. Nelson (QMUL, London)
Neal J. Turner (JPL-Caltech, Pasadena)
Colin P. McNally (NBIA, Copenhagen)
Udo Ziegler (AIP, Potsdam)

August 04-08, 2014
“Non-ideal MHD, Stability, and Dissipation in Protoplanetary Disks”

* oliver.gressel@nbi.dk

schematics of protostellar disc

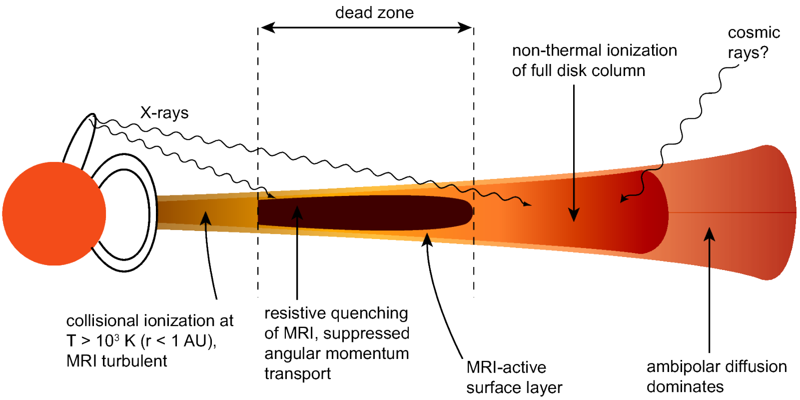

Armitage (2011)

play

embedded sub-disc

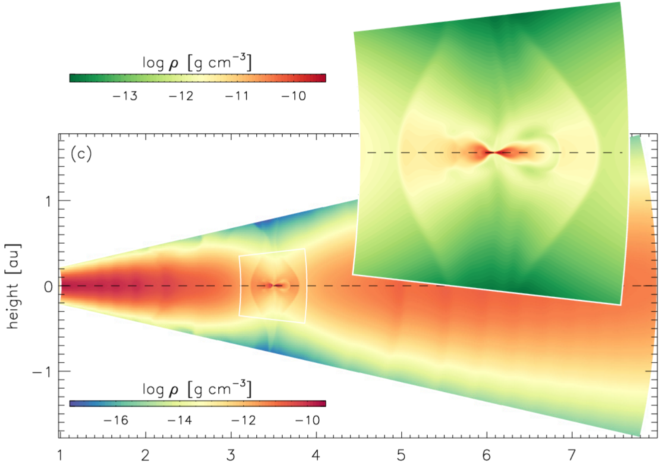

isothermal HD   non-isoth. HD   non-isoth. MHD

embedded sub-disc

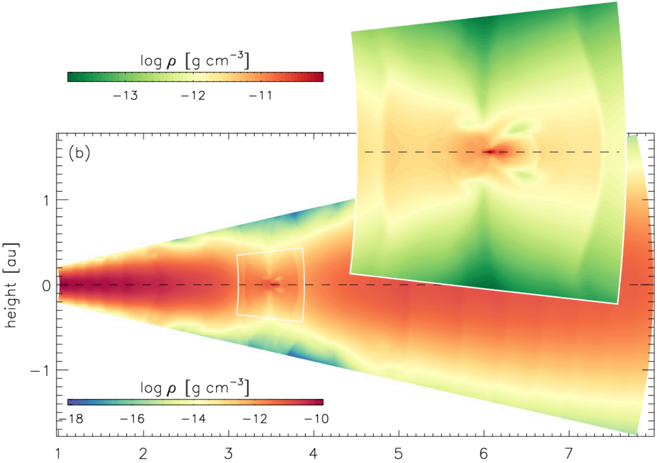

isothermal HD **non-isoth. HD** non-isoth. MHD

embedded sub-disc

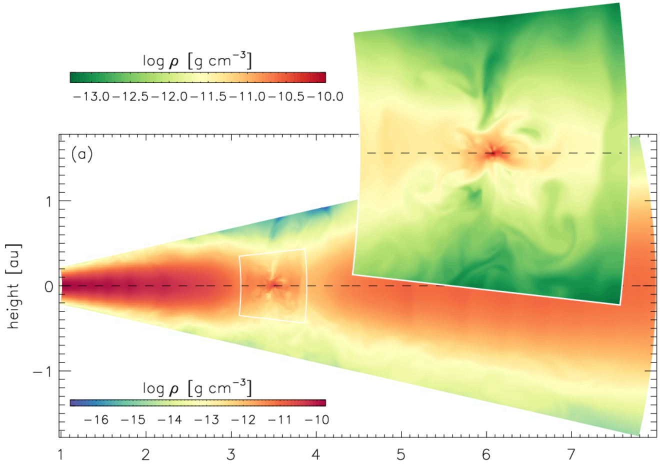

isothermal HD non-isoth. HD **non-isoth. MHD**

variability of circumplanetary disc

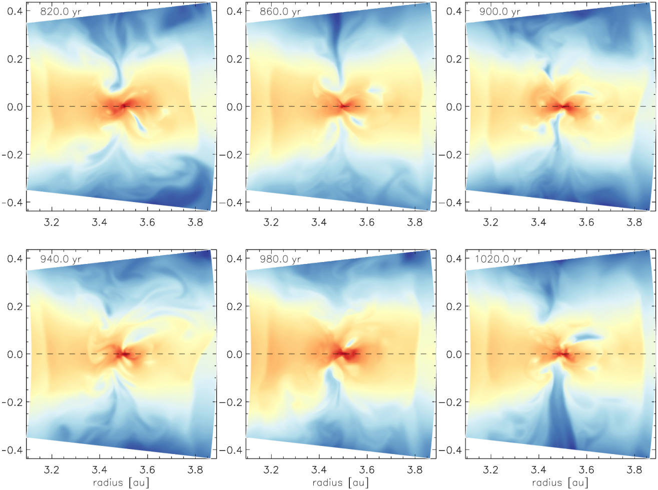

circum-jovian jet

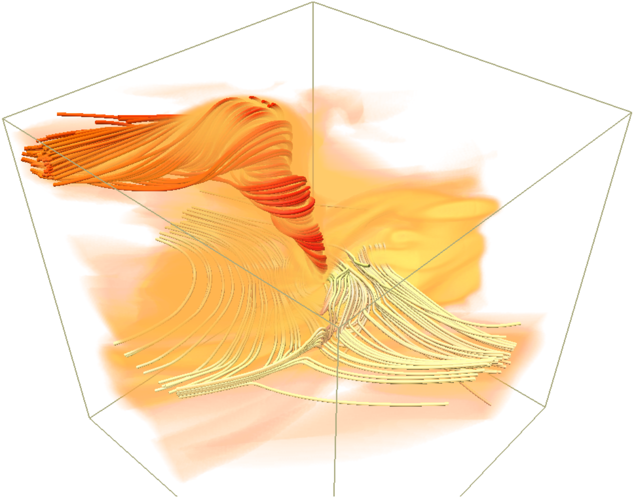

- Gressel et al. (2013), predicted by Quillen & Trilling (1998) and Fendt (2003), also cf. Machida et al. (2006)

revised schematics of protostellar disc

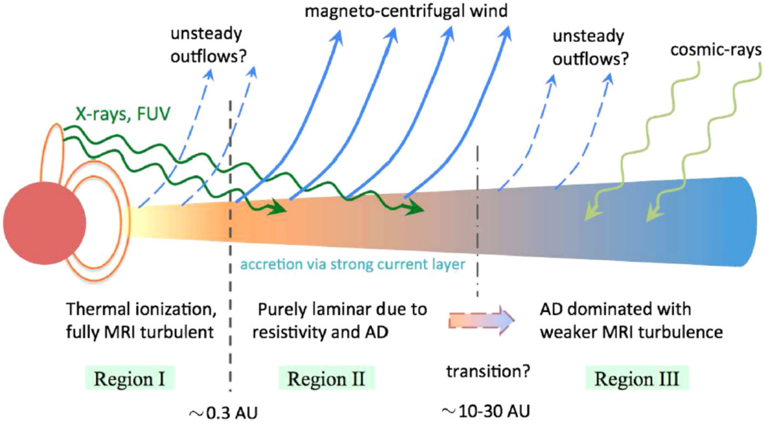

Bai & Stone (2013), Simon et al. (2013), Bai (2013), Kunz & Lesur (2013), Lesur, Fromang & Kunz (2014)

adding ambipolar diffusion

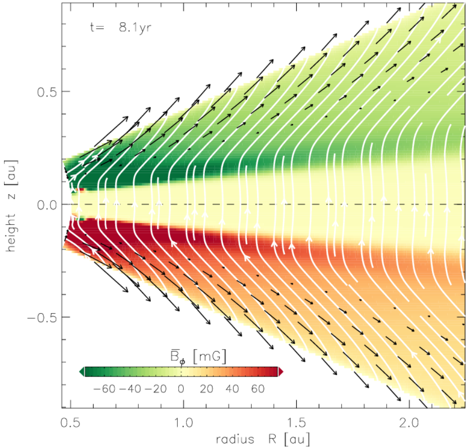

Gressel, Nelson, Turner & McNally (2014) in prep.
magneto-centrifugal wind from PPD with AD

- external ionisation
  via X-Rays, CRs, new: FUV layer
- Ohmic resistivity,
  new: ambipolar diffusion
- (no) magnetorotational instability (MRI)
  $\rightarrow$ (no) turbulent surface layers
- magneto-centrifugal (laminar) disc winds

- effect of reduced gas column in the gap region
- ionisation state of the CPD
- effect on jet launching

adding ambipolar diffusion

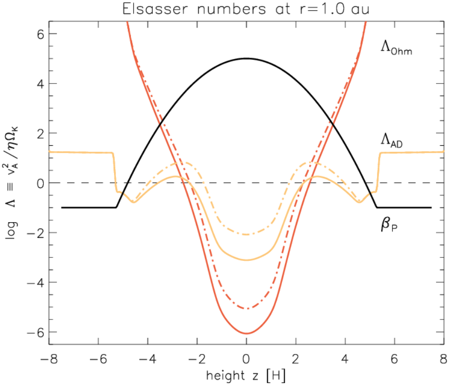

Gressel, Nelson, Turner & McNally (2014) in prep.
magneto-centrifugal wind from PPD with AD

- external ionisation
  via X-Rays, CRs, new: FUV layer
- Ohmic resistivity,
  new: ambipolar diffusion
- (no) magnetorotational instability (MRI)
  $\rightarrow$ (no) turbulent surface layers
- magneto-centrifugal (laminar) disc winds

- effect of reduced gas column in the gap region
- ionisation state of the CPD
- effect on jet launching

the fiducial model

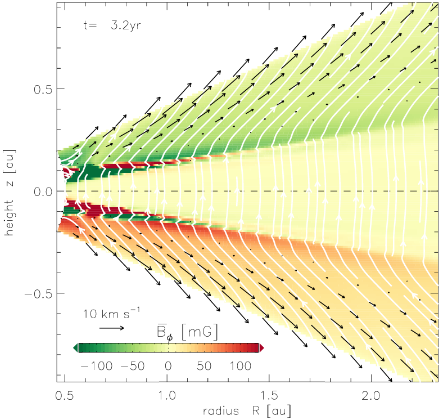

- MMSN disc model, NVF with midplane $\beta_{p\,0} = 10^5$, d/g mass ratio 10^{-3}, XR+CR+FUV

the fiducial model

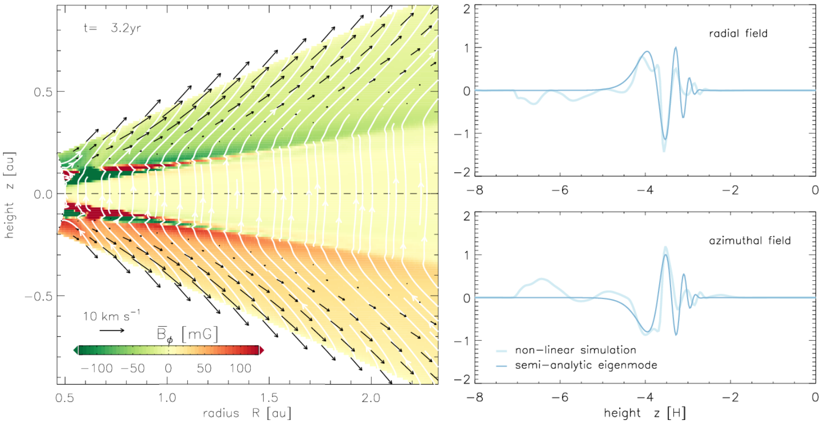

- MMSN disc model, NVF with midplane $\beta_{\mathrm{p}\,0} = 10^5$, d/g mass ratio 10^{-3}, XR+CR+FUV

the fiducial model

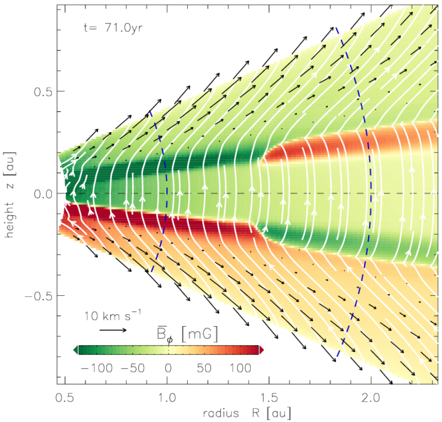

- MMSN disc model, NVF with midplane $\beta_{\rm p\,0} = 10^5$, d/g mass ratio 10^{-3}, XR+CR+FUV

the fiducial model

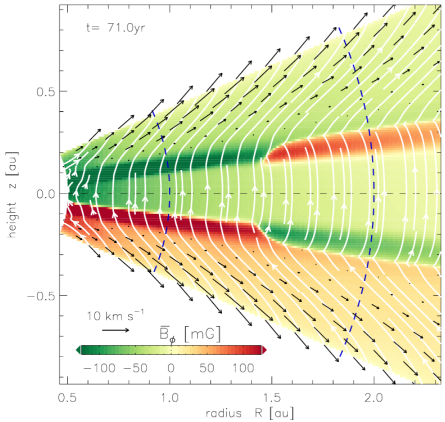

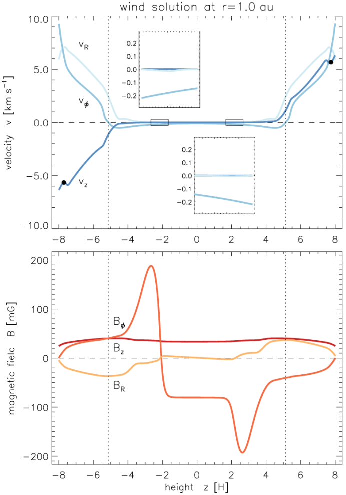

- MMSN disc model, NVF with midplane $\beta_{p\,0} = 10^5$, d/g mass ratio 10^{-3}, XR+CR+FUV

the fiducial model

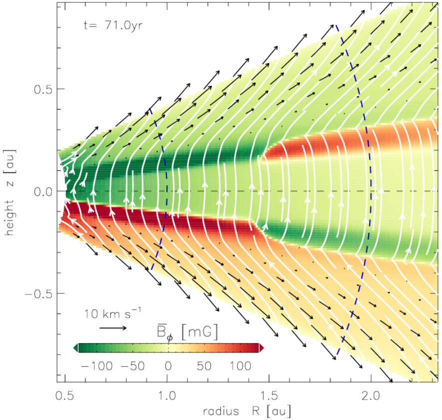

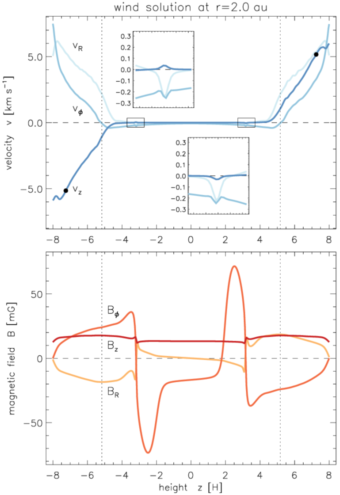

- MMSN disc model, NVF with midplane $\beta_{\mathrm{p}\,0} = 10^5$, d/g mass ratio 10^{-3}, XR+CR+FUV

collisional ionisation of inner disc

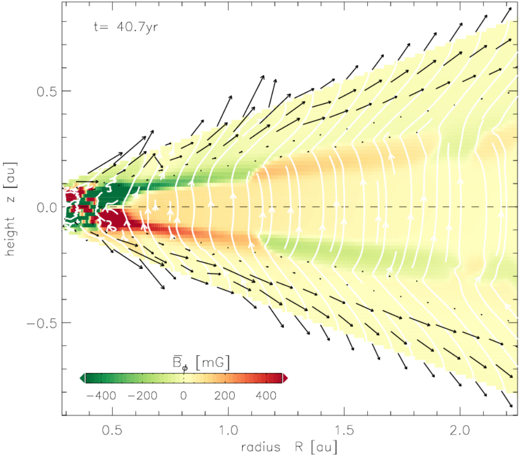

- MMSN disc model, midplane $\beta_{\mathrm{p}\,0} = 10^5$, d/g mass ratio 10^{-3}, XR+CR+FUV + thermal
- puffed-up turbulent disc shadows FUV radiation $\rightarrow$ variability/intermittency of disc wind

collisional ionisation of inner disc

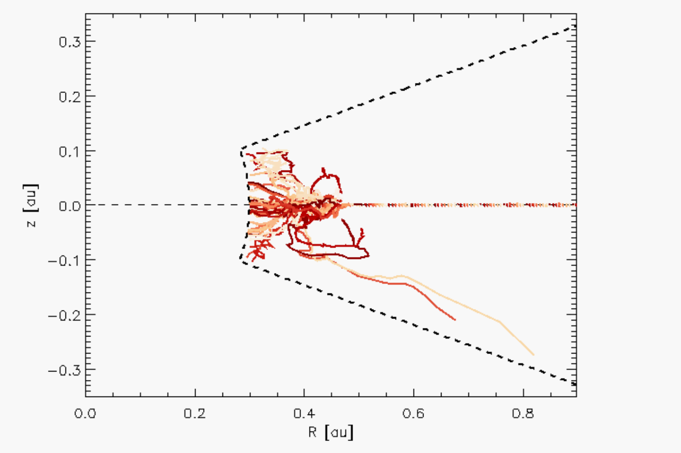

- MMSN disc model, midplane $\beta_{\mathrm{p}\,0} = 10^5$, d/g mass ratio 10^{-3}, XR+CR+FUV + thermal
- puffed-up turbulent disc shadows FUV radiation $\rightarrow$ variability/intermittency of disc wind

stability of current sheets

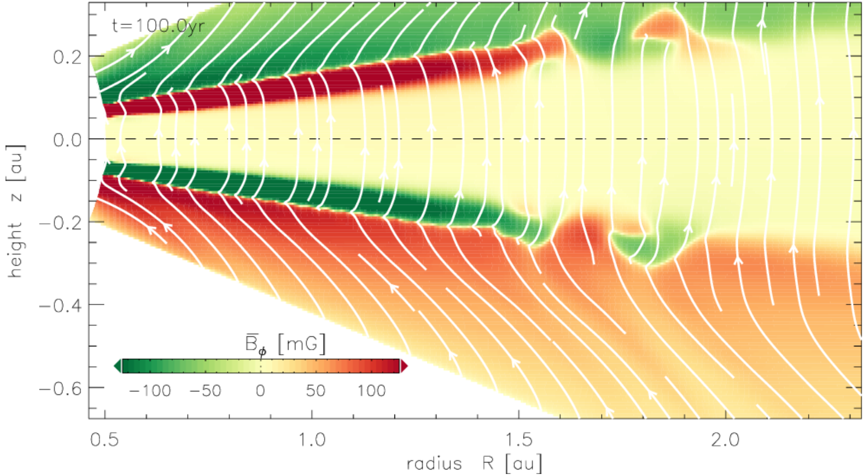

- flaring MMSN disc model, midplane $\beta_{p\,0} = 10^5$, d/g mass ratio 10^{-3}, XR+CR+FUV

stability of current sheets

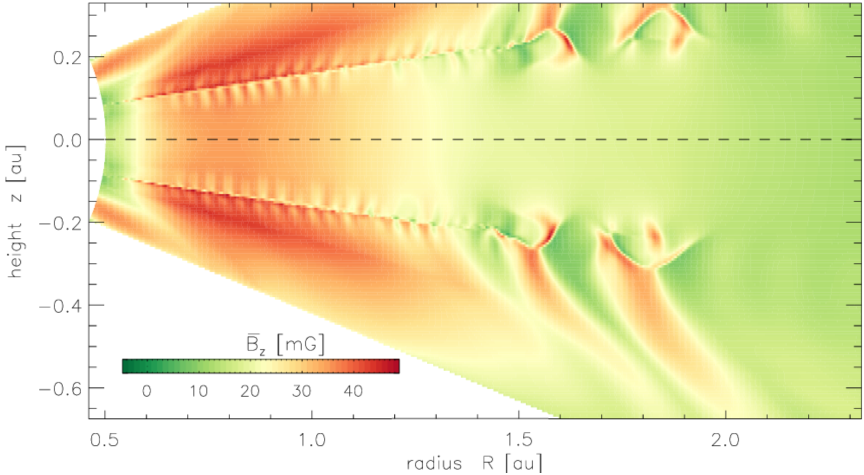

- flaring MMSN disc model, midplane $\beta_{\mathrm{p}\,0} = 10^5$, d/g mass ratio 10^{-3}, XR+CR+FUV

stability of current sheets

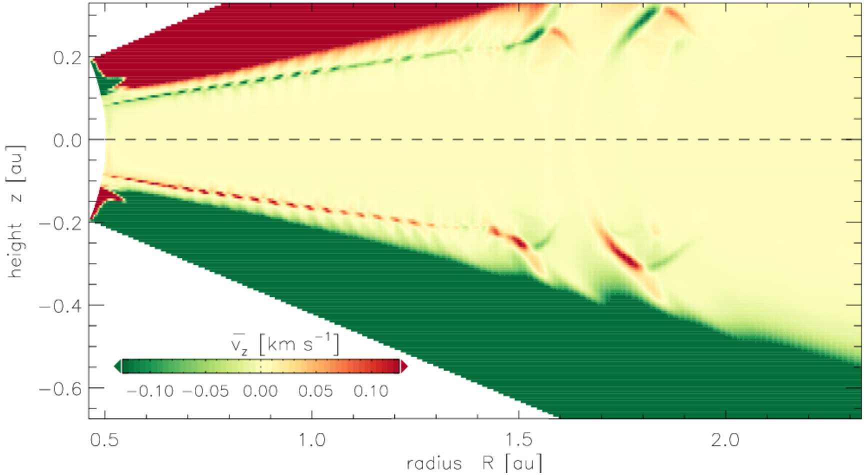

- flaring MMSN disc model, midplane $\beta_{\rm p\,0} = 10^5$, d/g mass ratio 10^{-3}, XR+CR+FUV

non-axisymmetric evolution

(flaring) MMSN disc with AD+Ohm   MMSN with Ohmic resistivity alone

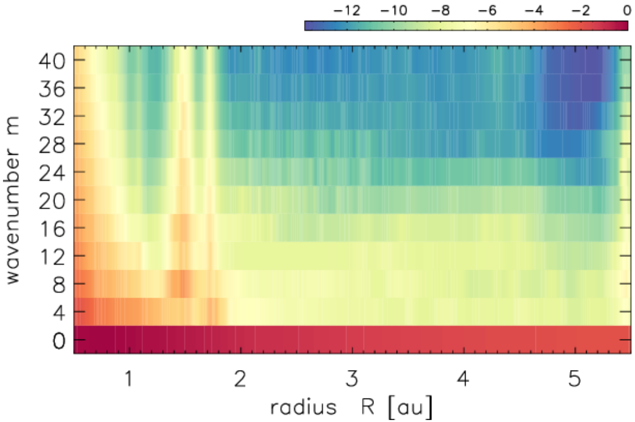

- flaring MMSN disc model, midplane $\beta_{\mathrm{p}\,0} = 10^5$, d/g mass ratio 10^{-3}, XR+CR+FUV

non-axisymmetric evolution

(flaring) MMSN disc with AD+Ohm MMSN with Ohmic resistivity alone

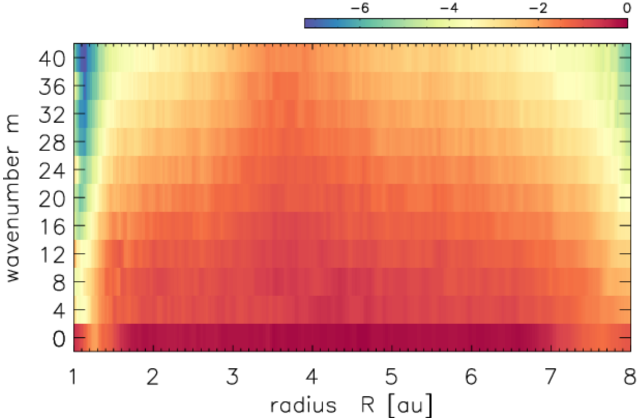

- flaring MMSN disc model, midplane $\beta_{p\,0} = 10^5$, d/g mass ratio 10^{-3}, XR+CR+FUV

reduced dust fraction

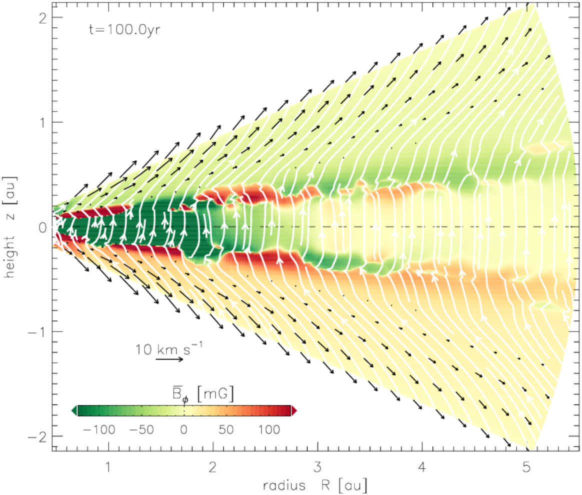

- MMSN disc model, midplane $\beta_{\mathrm{p}\,0} = 10^5$, d/g mass ratio 10^{-4}, XR+CR+FUV

shear-layer instability

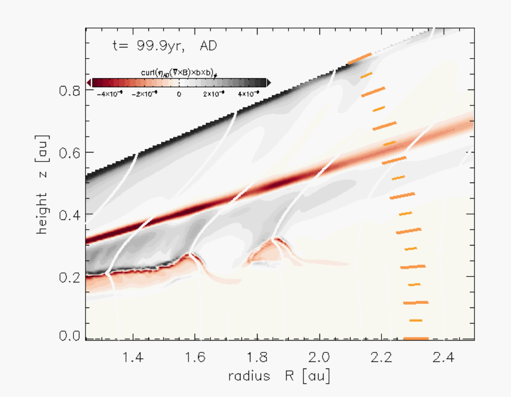

- velocity shear-layer at FUV transition – also seen in Bai & Stone (2013)
- most probably distinct from Moll (2012) “clumping” instability
- → coincidence of FUV transition and wind base, yes or no?!
- → need to control tapering of FUV transition?!

shear-layer instability

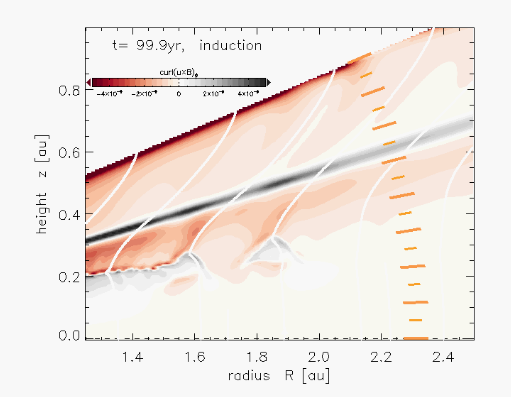

- velocity shear-layer at FUV transition – also seen in Bai & Stone (2013)
- most probably distinct from Moll (2012) “clumping” instability
- → coincidence of FUV transition and wind base, yes or no?!
- → need to control tapering of FUV transition?!

shear-layer instability

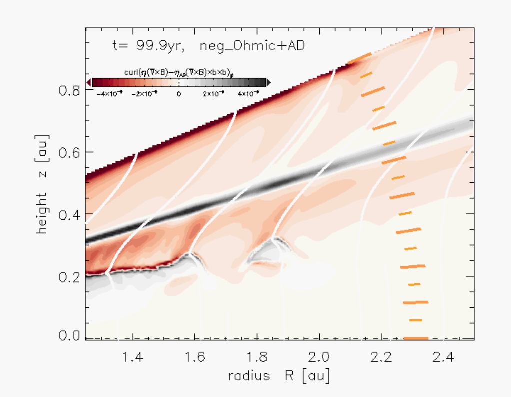

- velocity shear-layer at FUV transition – also seen in Bai & Stone (2013)
- most probably distinct from Moll (2012) “clumping” instability
- → coincidence of FUV transition and wind base, yes or no?!
- → need to control tapering of FUV transition?!

shear-layer instability

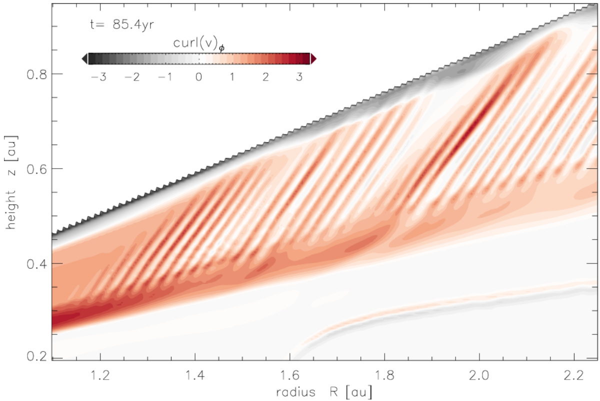

- velocity shear-layer at FUV transition – also seen in Bai & Stone (2013)
- most probably distinct from Moll (2012) “clumping” instability
- $\rightarrow$ coincidence of FUV transition and wind base, yes or no?!
- $\rightarrow$ need to control tapering of FUV transition?!

summary of simulation results

Table 2. Summary of simulation results.

	z_b [H]	z_A [H]	$T_{R\phi}^{\rm Reyn}$ [$10^{-6} p_0$]	$T_{R\phi}^{\rm Maxw}$ [$10^{-5} p_0$]	$T_{z\phi}^{\rm Maxw}$ [$10^{-5} p_0$]	$\dot{M}_{\rm wind}$ [$10^{-8} M_\odot {\rm yr}^{-1}$]	$\dot{M}_{\rm accr}$ [$10^{-8} M_\odot {\rm yr}^{-1}$]
O-b6	—	7.60 ± 0.45	6.87 ± 14.4	7.44 ± 0.95	—	1.47 ± 0.37	0.14 ± 1.53
OA-b5	5.23 ± 0.07	7.31 ± 0.17	3.63 ± 0.19	2.22 ± 0.06	9.82 ± 0.08	0.78 ± 0.01	0.43 ± 0.01
OA-b6	7.22 ± 0.48	6.94 ± 0.37	−0.21 ± 0.18	0.79 ± 0.06	0.58 ± 0.06	0.36 ± 0.03	0.08 ± 0.02
OA-b7	7.31 ± 0.70	6.39 ± 0.16	0.07 ± 0.13	< 0.01	0.22 ± 0.01	0.03 ± 0.01	0.00 ± 0.03
OA-b5-d4	5.27 ± 0.07	7.33 ± 0.18	0.11 ± 0.30	2.88 ± 0.11	9.88 ± 0.12	0.75 ± 0.01	0.33 ± 0.04
OA-b5-flr	4.81 ± 0.03	6.90 ± 0.31	0.26 ± 0.21	1.78 ± 0.02	14.3 ± 0.02	1.44 ± 0.01	0.64 ± 0.02
OA-b5-flr-nx	4.78 ± 0.03	7.50 ± 0.30	2.28 ± 9.24	1.87 ± 0.04	13.0 ± 0.04	1.31 ± 0.01	0.64 ± 0.03
OA-b5-nx	5.10 ± 0.04	7.34 ± 0.13	0.94 ± 9.29	1.89 ± 0.06	7.84 ± 0.02	0.66 ± 0.01	0.29 ± 0.03

The vertical position of the base of the wind, z_b, and the Alfvén point, z_A, are found independent on the radial location when measured in local scale heights, H. The viscous accretion stresses $T_{R\phi}$ are vertically integrated within $|z| \leqslant z_b$ – note the different units for Reynolds and Maxwell stresses. The wind stress, $T_{z\phi}$, is inferred at $z = \pm z_b$. All stresses depend weakly on radius; listed values are at $r = 3$ au.

summary of results

- First stratified global simulations of PPDs with Ohm+AD
  - proper wind geometry is naturally obtained
  - mass-loss rates agree with expectations from observations
- Long-term evolution and secondary instabilities
  - strong current sheets form adjacent to “un-dead” field belts
  - current layers break-up via tearing-mode (?!) instability
  - FUV transition drives (KH-unstable) velocity shear layer
- Future prospects
  - study time-variability induced by MRI-active inner disc
  - understand dependence of wind solution on input parameters
  - effect of AD within gap region / CPD evolution / core accretion
  - inclusion of Hall term / ...